Supporting Information

Near-room-temperature dielectric switch and thermal expansion anomaly in a new hybrid crystal: $(Me_2NH_2)[CsFe(CN)_5(NO)]$

Qi-Yao Li,[a] Mao-Fan Li,[a] Xiao-Xian Chen,[a] Ya-Ping Gong,[a] De-Xuan Liu,[a] Wei-Jian Xu,[a,b] Wei-Xiong Zhang[a]*

[a)] MOE Key Laboratory of Bioinorganic and Synthetic Chemistry, School of Chemistry, Sun Yat-Sen University, Guangzhou, 510275, China.
[b)] Department of Chemistry & CICECO-Aveiro Institute of Materials, University of Aveiro, 3810-193 Aveiro, Portugal.

Experimental

Synthesis

All chemicals were commercially available and used without further purification. The red block crystals of **1** were obtained by slow evaporation of an aqueous solution containing 0.482 g $Cs_2[Fe(CN)_5(NO)]$ and 0.326 g $Me_2NH{\cdot}HCl$ at room temperature for several days.

X-ray Crystallographic Analysis

The *in-situ* variable-temperature single-crystal X-ray diffraction data were collected on an Agilent SuperNova with graphite monochromated Mo *K*α radiation (λ = 0.71073 Å) in a temperature range of 250–320 K. The CrystalClear software package (Rigaku) was used for data collection, cell refinement, and data reduction. Using Olex^2 program, the structures were solved by using Intrinsic Phasing with the SHELXT structure solution program and using full-matrix least-squares method with the SHELXL refinement program.[S1,S2] The structures of LTP were refined using a racemic twinning matrix [−1 0 0 0 −1 0 0 0 −1] with BASF parameter. Non-hydrogen atoms were refined anisotropically and the positions of the hydrogen atoms were generated geometrically. The crystal data and structure refinement results at different temperatures for **1** are listed in Table S1.

Thermogravimetric analyses

Thermogravimetric analyses were carried out on a TA Q50 instrument in the temperature range of 298–1073 K at a heating rate of 10 K min^{-1} under a nitrogen atmosphere.

DSC measurements

Differential scanning calorimetry was carried out on a TA DSC Q2000 instrument under a nitrogen atmosphere in aluminum crucibles with heating and cooling rates of 10 K min^{-1} from 193 to 408 K.

Dielectric measurements

The dielectric measurement was carried on a TH2828A impedance analyzer for **1** under alternating current field with a voltage amplitude of 1.0 V and different frequences from 500 Hz to 2 MHz. The sample temperature was controlled in the range of 100–350 K with a temperature sweeping rate of 3 K/min approximately by a Mercury iTC cryogenic environment controller of Oxford Instrument. The powder sample of **1** was ground and pressed into tablets under a pressure around 5 GPa. The pressed-powder pellets were deposited with magnetic sheet used as electrodes.

Variable-temperature powder X-ray diffraction (PXRD)

Variable temperature PXRD patterns (Cu K_α, λ = 1.54178 Å) were collected on Bruker Advance D8 DA VANCI diffractometer for **1** in the temperature range of 223–353 K.

Hirshfeld surface analysis

Hirshfeld surfaces and the 2D-fingerprint plots were calculated with high resolution by CrystalExplorer[S3,S4] with inputting structure file in CIF format. The bond lengths related to hydrogen atoms were set to typical neutron values (C–H = 1.083 Å and N–H = 1.009 Å).

Table S1. Crystal data and structure refinement parameters for **1** at LTP and HTP.

Compound	**1**	
Formula	(Me_2NH_2) $[CsFe(CN)_5(NO)]$	
T (K)	250(2)	320(2)
Phases	LTP	HTP
Crystal system	orthorhombic	orthorhombic
Space group	$P2_12_12_1$ (No. 19)	*Bmmb* (No. 63)
a / Å	8.3288(3)	8.2860(3)
b / Å	8.9673(3)	9.0586(4)
c / Å	17.7852(7)	18.0168(7)
V / Å^3	1328.35(8)	1352.33(9)
Z	4	4
μ (mm^{-1})	3.832	3.764
F_{000}	752	752
R_{int}	0.0225	0.0225
Completeness (%)	100	100
Reflns. Collected	12283	6738
Independent reflns.	3607	1108
R_1[a] [$I > 2\,\sigma(I)$]	0.0204	0.0262
wR_2[b] [$I > 2\,\sigma(I)$]	0.0432	0.0671
R_1[a] (all data)	0.0229	0.0298
wR_2[b] (all data)	0.0443	0.0704
GOOF	1.042	1.093
BASF	0.09(3)	/

[a] $R_1 = \sum||F_o|-|F_c||/\sum|F_o|$; [b] $wR_2 = [\sum w(F_o^2 - F_c^2)^2/\sum w(F_o^2)^2]^{1/2}$.

Table S2. Selected inter-atomic distances (Å) for LTP and HTP.

LTP	Distance (Å)	**HTP**	Distance (Å)
Fe1-C1	1.936(4)	Fe1-C1	1.935(7)
Fe1-C2	1.945(3)	Fe1-C1'	1.915(7)
Fe1-C3	1.944(3)	Fe1-C2	1.939(5)
Fe1-C4	1.941(4)	Fe1-N3	1.643(4)
Fe1-C5	1.949(4)	Cs1-N1	3.259(7)
Fe1-N6	1.654(3)	Cs1-N1'	3.196(7)
Cs1-N1E	3.197(4)	Cs1-N2K	3.313(5)
Cs1-N2	3.255(3)	Cs1···N1L	3.754(9)
Cs1-N3F	3.299(3)		
Cs1-N4G	3.300(3)		
Cs1-N5H	3.215(4)		
Cs1···N1I	3.716(4)		
Cs1···N2J	4.915(3)		
Cs1···N4J	3.681(4)		
Cs1···N5I	3.749(4)		

Symmetry codes for LTP: E) −1+x, y, z; F) −1/2+x, 1/2−y, 1−z; G) x, −1+y, z; H) −1+x, −1+y, z; I) 1−x, −1/2+y, 1/2−z; J) −x, 1/2+y, 1/2−z. Symmetry codes For HTP: K) −1/2+x, −y,3/2-z; L) x, −y, 1−z;

Table S3. Hydrogen bonds for **1** at 250 K (LTP).

D	H	A	$d_{(D–H)}$ / Å	$d_{(H\cdots A)}$ / Å	$d_{(D\cdots A)}$ / Å	∠(D–H···A) /°
N7	H7a	N2	0.89	2.15	3.00	161.4
N7	H7b	N1F	0.89	2.42	3.20	146.7

Table S4. The cell parameters and *R*-factors in Pawley refinements on the variable-temperature powder X-ray diffraction patterns of **1**.

Phase	*T* (K)	*a* (Å)	*b* (Å)	*c* (Å)	*V* (Å^3)	R_p / %	R_{wp} / %
LTP	223(2)	8.349(1)	8.997(2)	17.778(2)	1335.3(2)	3.50%	5.28%
	243(2)	8.346(1)	8.993(1)	17.795(1)	1335.7(1)	3.71%	5.50%
	263(2)	8.339(1)	8.992(1)	17.812(1)	1335.8(3)	3.28%	5.01%
	273(2)	8.339(1)	8.991(1)	17.827(1)	1336.5(1)	3.43%	5.22%
	283(2)	8.333(1)	8.991(1)	17.838(1)	1336.5(1)	3.53%	5.33%
	293(2)	8.331(1)	8.990(1)	17.848(1)	1336.8(1)	3.45%	5.04%
HTP	303(2)	8.292(1)	9.071(1)	17.977(2)	1352.2(1)	3.68%	5.56%
	313(2)	8.295(1)	9.069(1)	17.996(2)	1354.0(1)	3.51%	5.34%
	333(2)	8.300(1)	9.072(1)	18.034(2)	1357.9(1)	3.31%	5.13%
	353(2)	8.303(1)	9.074(1)	18.073(2)	1361.7(1)	3.29%	5.06%

Table S5. The thermal expansion coefficients for **1**.

	Principal axes	α or β_V ($\times 10^{-6}$ K^{-1})	direction		
			a	*b*	*c*
LTP	X_1	−32(1)	−1	0	0
	X_2	−10(1)	0	1	0
	X_3	+56(1)	0	0	1
	V	+18(4)			
HTP	X_1	+7(2)	0	1	0
	X_2	+27(1)	−1	0	0
	X_3	+107(1)	0	0	1
	V	+142(1)			

α and β_V represent the axial and volumetric thermal expansion coefficients, respectively.

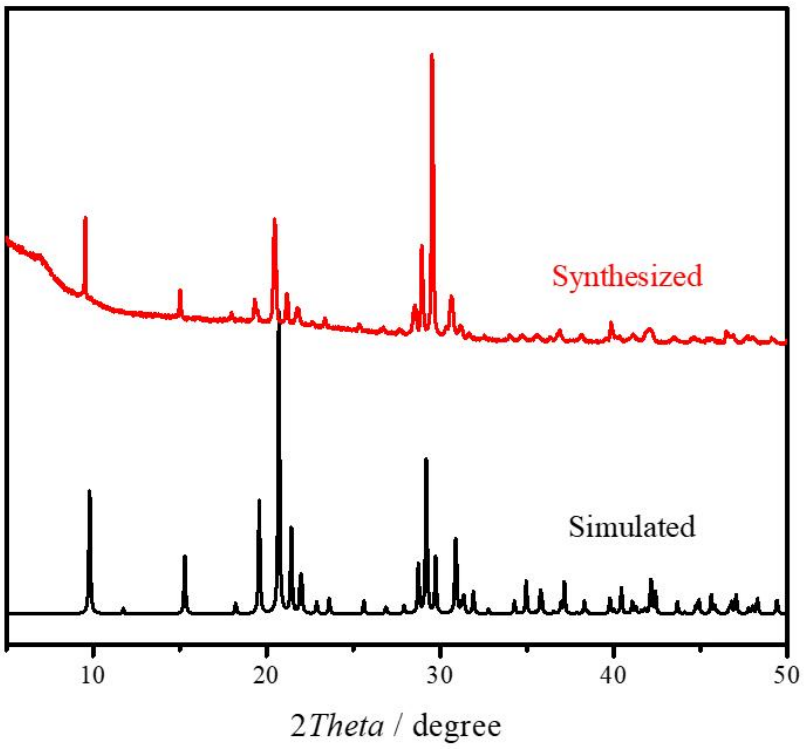

Figure S1. Experimental and simulated X-ray diffraction patterns for **1**.

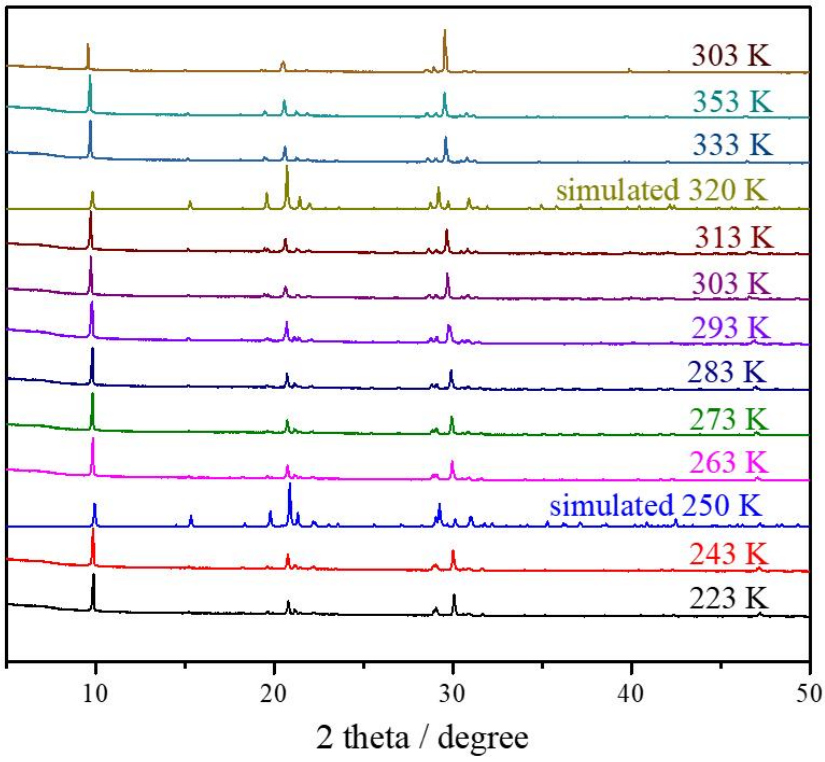

Figure S2. Variable-temperature powder X-ray diffraction patterns of **1**.

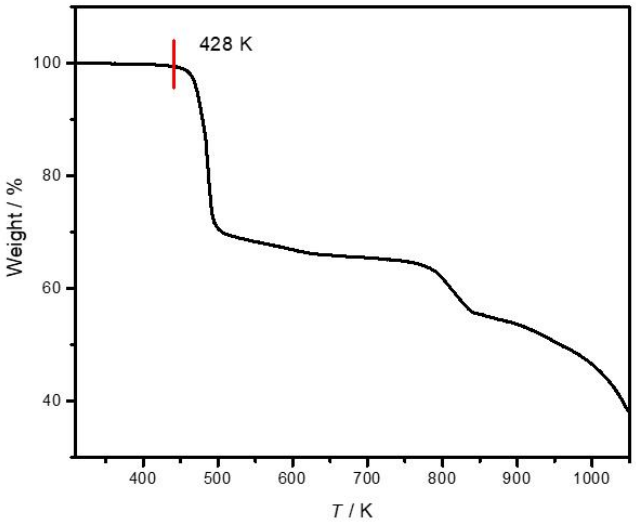

Figure S3. TG profile of **1**.

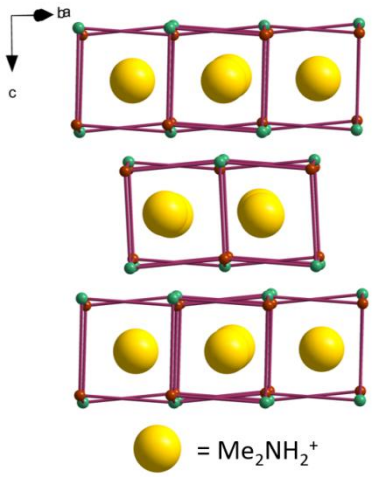

Figure S4. Perspective view of simplified structure **1** in LTP, linkages of cyano groups and $Me_2NH_2^+$ are depicted by purple lines and yellow spheres, respectively.

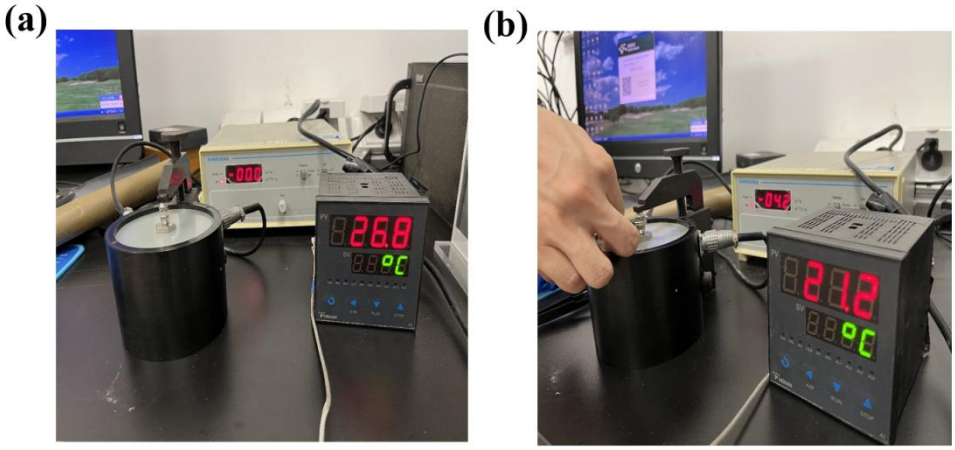

Figure S5. Piezoelectric test of **1**.

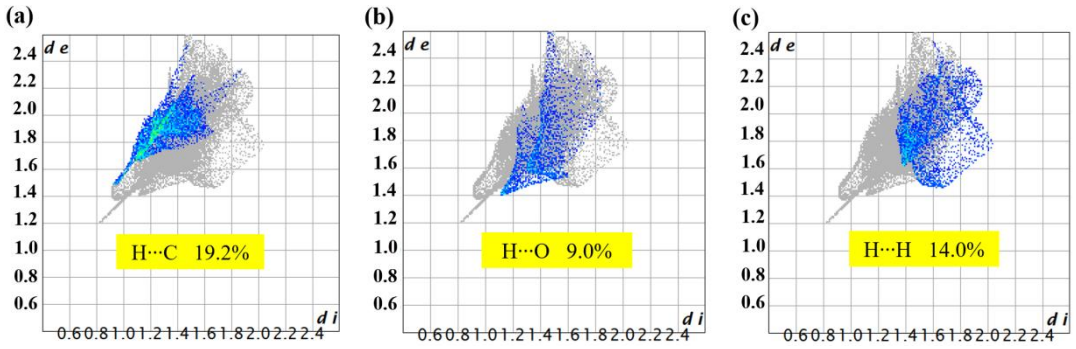

Figure S6. Fingerprint plots for H···C, H···O, and H···H contacts of Hirshfeld surface of organic cations in **1_LTP**.

References

[S1] O. V. Dolomanov, L. J. Bourhis, R. J. Gildea, J. A. K. Howard and H. Puschmann, *J. Appl. Cryst.*, 2009, **42**, 339-341.

[S2] G. M. Sheldrick, *Acta Cryst*., 2015, A71, 3-8.

[S3] M. A. Spackman and D. Jayatilaka, *CrystEngComm.*, 2009, **11**, 19-32.

[S4] P. R. Spackman, M. J. Turner, J. J. McKinnon, S. K. Wolff, D. J. Grimwood, D. Jayatilaka and M. A. Spackman, 2021, **54**, 1006-1011.